Nanosized Silica-Supported Metallocene/MAO Catalyst for Propylene Polymerization

Kuo-Tseng Li, Yi-Tyng Kao

Department of Chemical Engineering, Tunghai University, Taichung, Taiwan, Republic of China

Received 3 August 2005; accepted 10 December 2005
DOI 10.1002/app.23922
Published online in Wiley InterScience (www.interscience.wiley.com).

ABSTRACT: A nanosized silica particle was used as the support to prepare an Et[Ind]$_2$ZrCl$_2$/MAO catalyst for propylene polymerization of polypropylene. The catalyst and the polymer produced were characterized with nitrogen adsorption, ICP, DSC, SEM, TEM, XRD, solution viscometer, ^{13}C NMR and optical microscopy. The effects of polymerization temperature and [Al]/[Zr] ratio on catalyst activity and polymer melting point were investigated. Under identical reaction conditions, nanosized catalyst exhibited better polymerization activity than the microsized catalyst (e.g., the former had 64% higher activity than the latter at the optimum polymerization temperature (50°C) and [Al]/[Zr] = 570). DSC results indicated that polymer melting point increased with the increase of [Al]/[Zr] ratio and with the decrease of polymerization temperature. XRD results showed that the percentage of γ crystals increased with decreasing [Al]/[Zr] ratio. Electron microscopic results showed that the polymer particle size increased with increasing polymerization temperature. © 2006 Wiley Periodicals, Inc. J Appl Polym Sci 101: 2573–2580, 2006

Key words: isotatic polypropylene; propylene polymerization; nano silica particles; supported metallocene/MAO catalyst

INTRODUCTION

Polypropylene (PP) is one of the leading polymers with the present annual world demand of around 40 million tons. It is a versatile polymer and is widely used in automotive and electrical components, consumer products (e.g., kitchen wares, tray, toys, and packing materials), fibers (especially in carpet), and films.[1–3] Commercial isotactic PP is traditionally produced in a continuous slurry reactor or in a gas fluidized bed reactor, using $MgCl_2$ supported Ziegler–Natta catalysts.

In 1985, Kaminsky et al.[4] obtained highly isotactic PP by using a chiral zirconocene (*rac*-Et(Ind)$_2$ZrCl$_2$) and methylaluminoxane (MAO) as cocatalyst. Metallocene-based catalyst systems are dramatically different from Ziegler–Natta catalysts, because they have much higher activity and lower polydispersity.[5] To solve the problems observed with the soluble homogeneous catalysts (including the difficulty in controlling the polymer morphology, the very large amount of MAO needed, and the reactor-fouling problem), heterogenization of the metallocenes is crucial for industrial application.[6–12] The development of supported metallocenes enables their use in gas- and slurry-phase processes and prevents reactor-fouling problems. It also enables the formation of uniform particles with narrow size distribution and high bulk density. In addition, supported systems need a much smaller [Al]/[Zr] ratio than homogeneous systems. To obtain the maximum activity, [Al]/[Zr] ratio was decreased from 3000 to 100,000 for the homogeneous catalysts to 100–500 for the heterogeneous catalysts, probably because MAO had the lower deactivation rate when one side is blocked by the support.[11]

Silica is one of the most frequently used supports, because it leads to good morphological features for polymer particles. Three methods were commonly used to immobilize metallocenes on silica[11,13,14]: (a) adsorption of metallocenes onto a MAO-pretreated silica support; (b)reacting silica with a metallocene/MAO mixture; (c)supporting the metallocene and then reacting with MAO.[15] The most common industrial method is to treat the support with MAO first and then adsorb the metallocene on it (i.e., method a). In the literature, the sizes of silica particles used to support metallocene/MAO catalysts for propylene polymerization to polypropylene were usually in the range of micrometers or more.

In this study, we used a nanosized silica particle as the support for metallocene/MAO catalyst. We found that the nanosized catalyst system exhibited significantly better propylene polymerization activity than the microsized catalyst system under identical reaction conditions.

Correspondence to: K.-T. Li (ktli@thu.edu.tw).
Contract grant sponsor: National Science Council, Republic of China; contract grant number: NSC-93–2214-E029–002.

EXPERIMENTAL

Catalyst preparation and characterization

The supported metallocene/methylaluminoxane (MAO) catalyst was prepared using method (a) mentioned in the Introduction section,[16] according to the following procedure: (1) calcination of silica particles at 450°C under a nitrogen flow (100 mL/min) for 3 h, (2) immobilization of MAO on the supports by heating 7 mL of 10 wt % MAO solution (in toluene) with 1 g silica particle at 50°C for 24 h, followed by washing with toluene three times, (3) reaction of the MAO-treated supports with metallocene compounds (0.072 g rac-ethylenebis(1-indenyl)zirconium (IV) dichloride, *rac*-Et[Ind]$_2$ZrCl$_2$) at 70°C for 16 h, followed by washing with toluene three times, (4) drying the catalyst at 50°C. The operations of steps (2)–(4) were carried out under a dry argon atmosphere by using glove-box technique. Two silica sources were used as the support for metallocene/MAO catalyst. One silica was nanosized, supplied by SeedChem (Melbourne, Australia); another silica was microsized, supplied by Strem (Newburyport, MA). *rac*-Et[Ind]$_2$ZrCl$_2$ and MAO (10 wt % solution in toluene) were supplied by Aldrich (St. Louis, MO) and Albemarte (Baton Rouge, LA), respectively.

The specific surface areas and the pore size distributions of the silica samples were determined by nitrogen adsorption at the temperature of liquid nitrogen with a Micrometrics Brunauer-Emmett-Teller (BET) surface area analyzer (Model ASAP 2020). Zirconium and aluminum contents of the resulting supported metallocene/MAO catalysts were determined with an inductively coupled plasma-atomic emission (ICP-AES) spectrometer (Kontron, Model *S*-35) after HF acid digestion of the solid. Transmission electron microscopy (TEM) observations were made using JEOL JEM-2010. Scanning electron microscopy (SEM) experiments were carried out with a JEOL SEM (model JSM-6700F).

Propylene polymerization and polymer characterization

A 100-mL high-pressure autoclave reactor (supplied by Parr Instrument) equipped with an impeller and a temperature control unit was employed for carrying out the catalytic polymerization of propylene. The autoclave was heated by a thermoregulated oven and a thermocouple was used to monitor the reaction temperature. In a typical experiment, 50 mL toluene, a prescribed amount of supported metallocene/MAO catalysts (prepared by impregnation method mentioned above) and MAO solution (if any) were charged to the reactor. The reactor was heated or cooled to the desired temperature (the temperature was set in the range of 2–70°C). Propylene at 100 psi was then introduced into the reactor to initiate the polymerization and the propylene pressure was maintained constant at 100 psi. The agitator speed was set at 350 rpm and the reaction time was 2 h. The polymerization was then terminated by adding methanol and the polymer product was dried in a vacuum oven. The measured polymer weight was used for determining the polymerization activity, according to the following equation: polymerization activity = (kilograms of PP)/(polymerization time $\times$ moles of Zr in the catalyst).

The polymers produced were characterized with X-ray diffraction (XRD), SEM, optical microscope, DSC, solution viscometer, and ^{13}C NMR. Polymer particle morphology was observed using a scanning electron microscope (JEOL JSM-5400). Polymer crystal structure was examined by XRD crystallography on a Shimadzu XRD-6000 diffractometer with Cu Kα radiation. The DSC measurements for the determination of the melting point were carried out on a differential scanning calorimeter (PerkinElmer Pyris–1) with a heating rate of 5°C/min. The structure of the melt-crystallized polymer was observed with an optical microscope (Nikon E400) in cross-polarized light. The fraction of *mmmm* pentad in polymer was evaluated from quantitative ^{13} C NMR spectra, which was recorded with a Varian UNITY-600 NMR spectrometer at 100°C with *o*-$C_6D_4Cl_2$ as the solvent. Polymer molecular weight was determined with solution viscosity method. The intrinsic viscosity [η] of the dried polymer was measured with a Schott AVS 300 system at 135°C with *o*-$C_6H_4Cl_2$ as the solvent. The viscosity–average molecular weight ($\bar{M}_v$) was calculated from the intrinsic viscosity data using the Mark–Houwink equation ($[\eta] = K\bar{M}_v^{\alpha}$) for isotatic polypropylene with $K = 1.3 \times 10^{-4}$ dL/g and $\alpha = 0.78$.[17]

RESULTS AND DISCUSSION

Catalyst characterization

Two silica sources were used as the support for Et[Ind]$_2$ZrCl$_2$/MAO catalysts. One silica was nanosized and another silica was microsized. Figure 1 shows the TEM of the nanosized silica particle (silica particles are shown in the dark areas), which indicates that most particles had a slender shape with a length of around 10 nm and a width in the range of 2–4 nm. Figure 2 shows the SEM of the microsized silica, which had a diameter of around 100 μm.

Table I reports the results of ICP measurements for the supported catalysts. Zr and Al contents of the nanosized catalyst were 1.09 and 5.37 wt %, respectively, which were only slightly higher than those of the microsized catalyst (0.95 wt % Zr and 4.86 wt % Al). The [Al]/[Zr] ratio was essentially the same ($\sim$17) for the two catalysts. BET measurements indicated

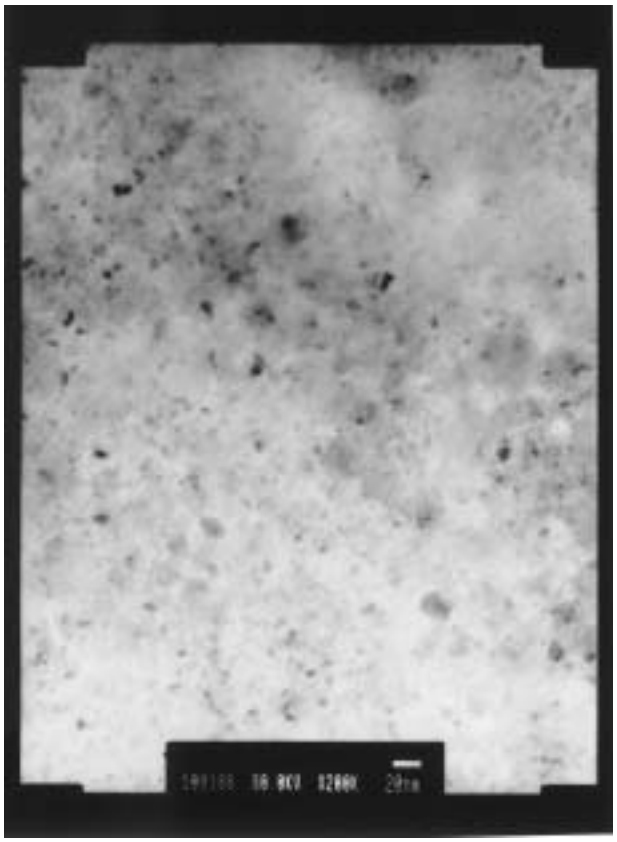

Figure 1 TEM picture of the nanosized silica particles.

that the surface area of the nanosized slica was 582 m^2/g, which was 1.9 times that of the microsized silica (surface area = 305 m^2/g).

The nanosized catalyst had higher (~10% higher) Al content than the microsized catalyst; however, the Al concentration (expressed in terms of g Al/m^2 calculated from the results of ICP and BET measurements)

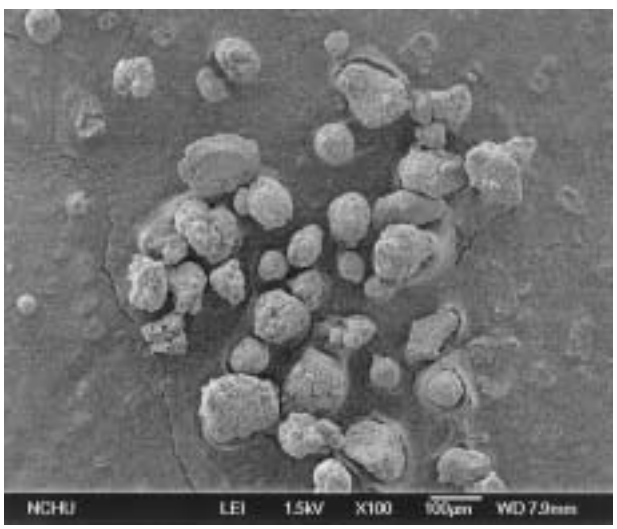

Figure 2 SEM picture of the microsized silica particles.

TABLE I
Zr Content, Al Content, and [Al]/[Zr] Ratio for the Silica-Supported Metallocene/MAO Catalysts

Catalyst	Zr content (wt %)	Al content (wt %)	[Al]/[Zr]
Nanosized	1.09	5.37	16.6
Microsized	0.95	4.86	17.2

of the nanosized catalyst was only 0.58 times that of the microsized catalyst. It was known that MAO is immobilized on the silica through the following reaction[18]:

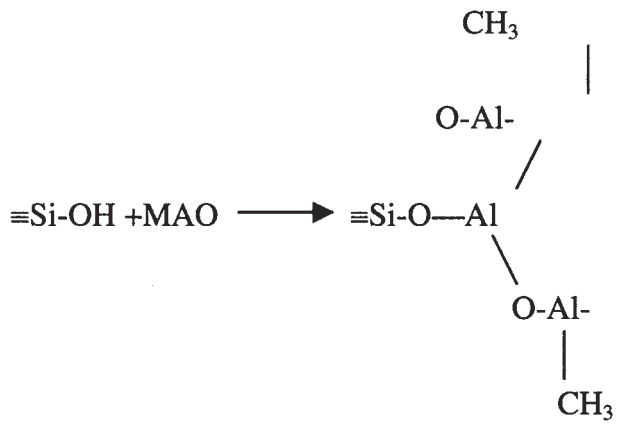

I (1)

where MAO is a complex mixture of linear and cyclic oligomeric aluminoxanes having molecular weight from 1200 to 1600 and containing 20–30 wt % trimethylaluminum (according to the specifications of the MAO supplier). For silica gel treated at 450°C, the surface concentration of silanol groups (≡SiOH) on silica gel was around 4 $\mu mol/m^2$.[19] The lower Al concentration observed for the nanosized catalyst indicated that significant amounts of surface silanol groups on the nanosized silica did not react with MAO. This should be due to the stronger diffusion limitation effect in the nanosized silica particle, which prevented some of the internal SiOH groups from reacting with the MAO molecule.

The extent of diffusion limitation of MAO molecules inside a silica gel pore is determined by the pore size of silica gel. The pore size distributions of the nanosized slica particles and the microsized silica particles are shown in Figures 3 and 4, respectively. Figure 3 indicates that most of the pores in the nanosized silica particles were very small (diameter $\leqq$ 2.5 nm). Figure 4 indicates that most of the pores in the microsized silica particles were in the range of 10–30 nm, with an average pore diameter of 21 nm. Some pores in the

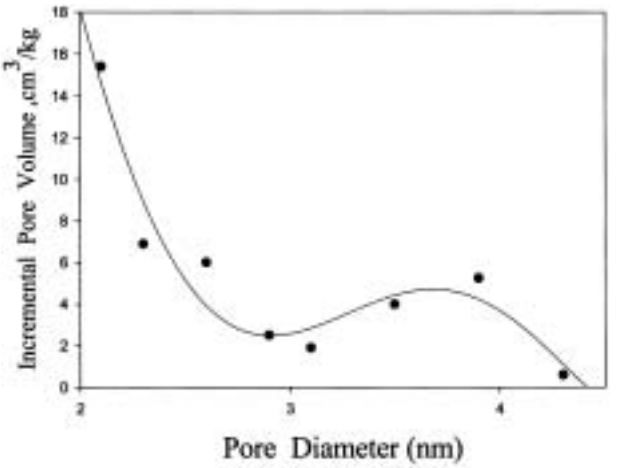

Figure 3 Pore size distribution of the nanosized silica particles.

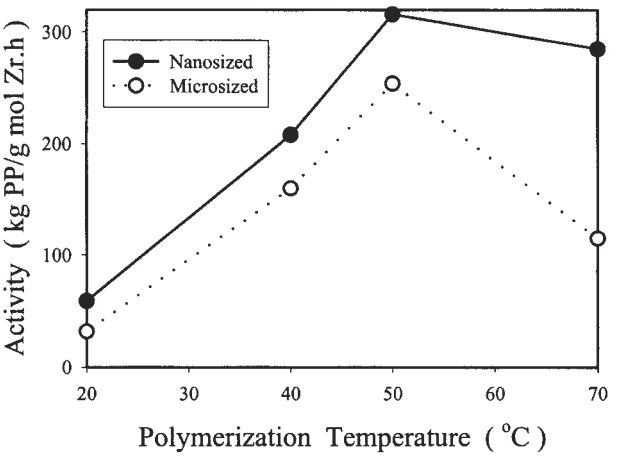

Figure 5 Polymer activity as a function of polymerization temperature for the nanosized and the microsized catalysts([Al]/[Zr] = 17, polymerization time = 2 h).

nanosized slica were too small for the MAO molecules to enter, and therefore, the SiOH groups in these small pores did not react with MAO. The much smaller pores in the nonosized silica (compared to those in the microsized silica) should be the major reason that the nonosized silica had the lower Al concentration than the microsized catalyst.

Propylene polymerization

The nanosized silica and the microsized silica supported Et[Ind]$_2$ZrCl$_2$/MAO catalysts prepared above were used to study the polymerization of propylene to polypropylene under two [Al]/[Zr] ratios: [Al]/[Zr] = 17 (i.e., without the addition of external MAO in the reaction mixture) and [Al]/[Zr] = 570 (i.e., with the addition of external MAO solution in the reaction mixture). The effect of polymerization temperature on the polymerization activity was investigated and the experimental results for [Al]/[Zr] = 17 and 570 are shown in Figures 5 and 6, respectively. It can be clearly seen from Figures 5 and 6 that the nanosized catalyst had significantly better polymerization activity than the microsized catalyst in the temperature range of 20–70°C.

The effects of polymerization temperature on polymerization activity were similar for both the nanosized and the microsized catalysts. All the curves in Figures 5 and 6 exhibit a volcano shape with a maximum polymerization activity at the polymerization temperature of 50°C. In Figure 5, the maximum polymer activities obtained for the nanosized catalyst and the microsized catalyst were 317 kg PP/mol Zr h and 254 kg PP/mol Zr h, respectively. In Figure 6, the maximum polymerization activities obtained for nanosized catalyst and microsized catalyst were 3824 kg PP/mol Zr h and 2325 kg PP/mol Zr h, respec-

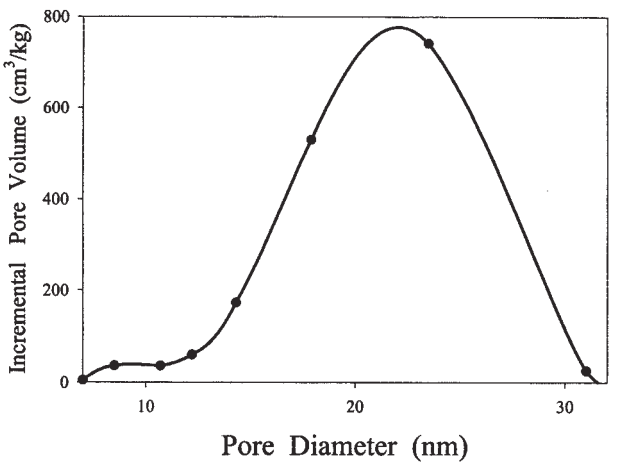

Figure 4 Pore size distribution of the microsized silica particles.

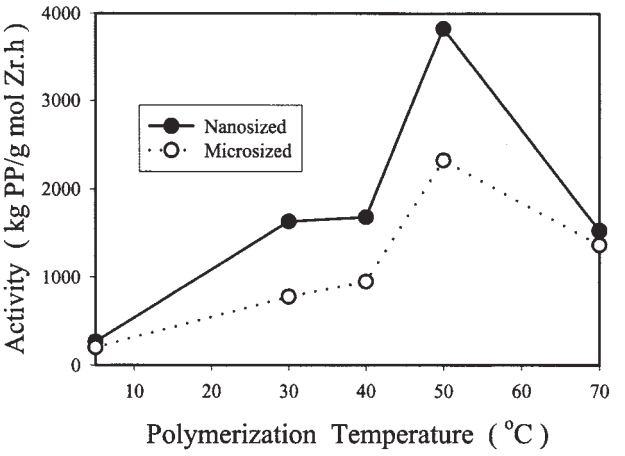

Figure 6 Polymerization activity as a function of polymerization temperature ([Al]/[Zr] = 570, polymerization time = 2 h).

tively. These maximum activities shown in Figure 6 were 12-fold and ninefold of those corresponding activities shown in Figure 5. Therefore, the presence of external MAO resulted in a marked increase of the polymerization activity. Figure 6 indicated that the maximum activity obtained (at 50°C) with the nanosized catalyst was 1.64 times that obtained with the microsized catalyst.

When the polymerization temperature was $\leqq$ 50°C, the polymerization activity of both catalysts increased monotonically with the polymerization temperature (Figs. 5 and 6). Further increase in the polymerization temperature resulted in the decrease of polymerization activity. The polymerization rate R_p is related to the concentration of the catalytically active species [C*] and propylene concentration [M] according to the following equation[20]:

$$R_P = k_P[C^*][M] \tag{2}$$

where k_p is the apparent polymerization rate constant. Therefore, the observed polymerization activity (shown in Figs. 5 and 6) should be determined by k_p, [C*], and the solubility of propylene in toluene [i.e., [M] in eq. (2)]. It is known that the solubility of propylene in toluene decreased linearly with the increase of temperature.[21] The concentration of the catalytically active species [C*] in eq. (2) is related to the material balance of all zirconcene species, according to the following equation[20]:

$$[C^*]+2[C2]+[C—MAO]+[C_d]=[Zr] \tag{3}$$

where C2 and C—MAO are two types of inactive species, which are in dynamic equilibrium with C*, C_d is the dead species resulting from irreversible catalyst deactivation. With the increase of polymerization temperature, k_p increased but both [M] and [C*] decreased. When the polymerization temperature was $\leqq$ 50°C, k_p increased more rapidly than the decrease of [C*] and [M], which resulted in the increase of the observed polymerization activity. When the polymerization temperature was above 50°C, the extents of [C*] and [M] decrease were more profound than the extent of k_p increase, which resulted in the decrease of the observed polymerization activity, as shown in Figures 5 and 6.

Comparisons of Figures 5 and 6 indicate that the presence of external MAO resulted in a dramatic increase of the polymerization activity. The increase of the polymerization activity observed in Figure 6 should be due to the increase of the metallocene catalyst activation process caused by the large excess of MAO. The external added MAO should involve in the increase of the rate of the activation of the species II in the following equation[18]:

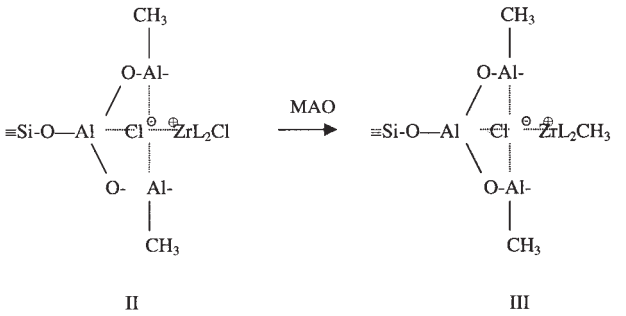

(4)

where L is ligand framework and species III is the catalytically active species. The species II in eq. (4) was formed from the adsorption of metallocene on the MAO-mediated silica [formed in eq. (1)], according to the following equation[18]:

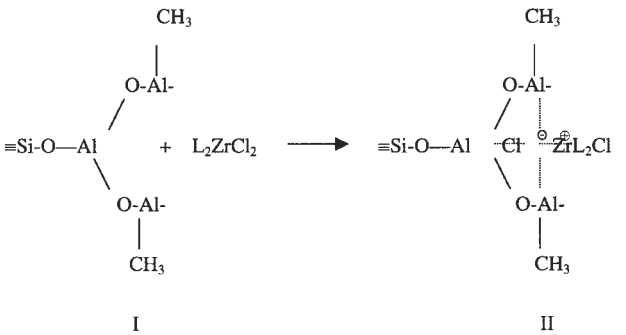

(5)

The effect of polymerization temperature on polymerization activity shown in Figure 5 (without the addition of external MAO) was similar to that shown in Figure 6 (with the addition of external MAO). The similarity suggests that the reaction presented in eq. (5) was not affected by the presence of the external added MAO. In other words, only MAO bonded to silica gel participated in the formation of the species I in eq. (1).

Polymer characterization

Figure 7 shows the effects of polymerization temperature (T_p) and [Al]/[Zr] ratio on the polymer melting point (T_m) for the nanosized catalyst, which were obtained from DSC measurements. T_m provides information about the polymer molecular weight and the microstructure of the polymer molecules. As shown in Figure 7, the increase of polymerization temperature strongly reduced the melting points of the polymers, which should be caused by the decrease of the molecular weight and the isotacticity of the polymer produced. Figure 8 shows that the viscosity–average molecular weight decreased rapidly with the increase of polymerization temperature ($\bar{M}_v$ = 33,240 g/mol at T_p = 20°C, and $\bar{M}_v$ = 6780 g/mol at T_p = 70°C when [Al]/[Zr] = 570). The decrease of molecular weight

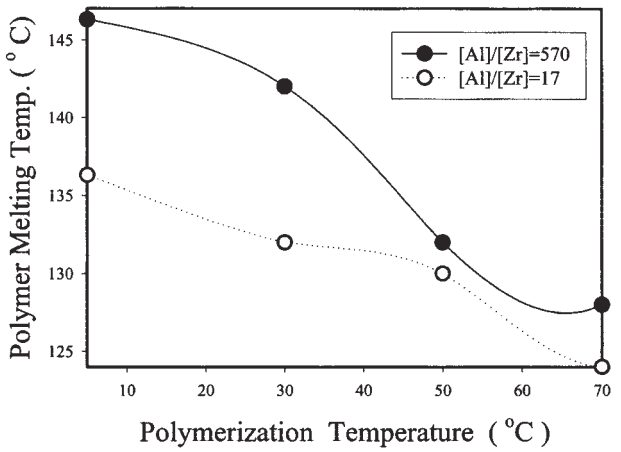

Figure 7 Effects of polymerization temperature and [Al]/[Zr] ratio on the polymer melting point.

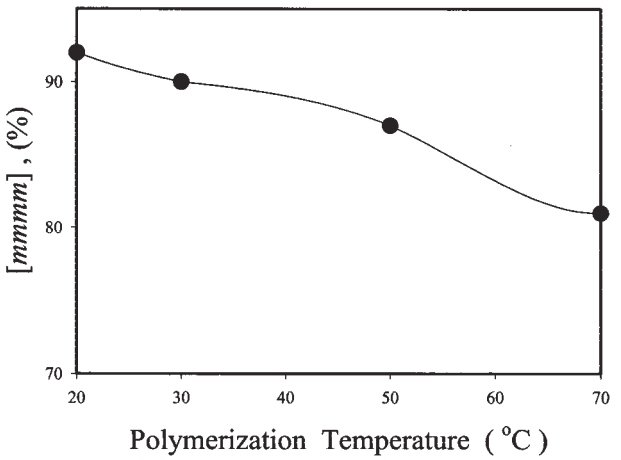

Figure 9 Effect of polymerization temperature on the content of *mmmm* pentads in the polypropylene samples obtained ([Al]/[Zr] = 570).

with the increase of polymerization temperature was due to the enhanced chain-transfer reaction (because the activation energy for chain transfer reaction is greater than the activation for propagation reaction). The polypropylene tacticity was calculated by ^{13}C NMR. Figure 9 shows the effect of polymerization temperature on the content of *mmmm* pentads in the polypropylene samples obtained, which indicated that the percent *mmmm* pentads decreased from 92% at T_p = 20°C to 82% at T_p = 70°C. The decrease of the stereoregularity of the polymer was caused by the lower probability of a "correct" monomer insertion in the enantiomorphic site at elevated temperature.[22] Comparisons of the data in Figures 8 and 9 suggest that polymerization temperature has stronger effect on the polymer molecular weight than on the polymer isotacticity. Therefore, polymer molecular weight should be the main factor that caused the decrease of the polymer melting temperature.

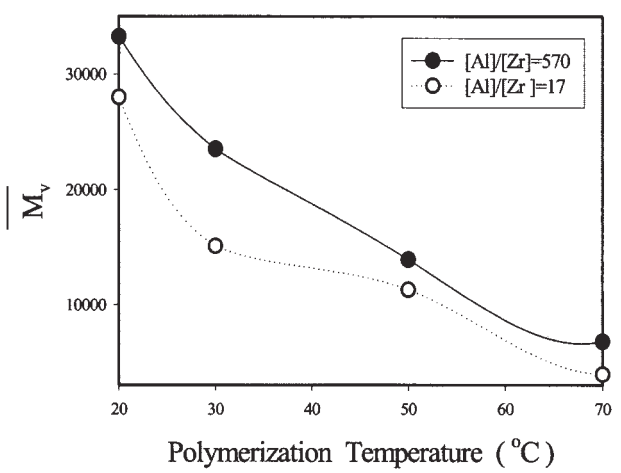

Figure 8 Effects of polymerization temperature and [Al]/[Zr] ratio on the viscosity–average molecular weight M_v of the polymer.

Figure 7 also shows that an increase of MAO concentration ([Al]/[Zr] ratio increased from 17 to 570) resulted in the significant increase of the polymer melting point. This is opposite to that observed for the homogeneous metallocene catalyst system, where the increase of [Al]/[Zr] ratio resulted in the decrease of polymer melting point. For the homogeneous metallocene catalyst system, the decrease of molecular weight with the increase of [Al]/[Zr] ratio was due to the chain transfer to trimethylaluminum (TMA) present in the MAO solution.[23] The results in Figure 7 suggests that the chain transfer to aluminum might be reduced markedly for the supported metallocene catalysts. The lower polymer melting points observed with the lower [Al]/[Zr] might also be due to its lower isotacticity, as shown from the XRD analyses (the results of XRD studies will be presented later in Figs. 12 and 13).

Figures 10 and 11 show SEM pictures of the polypropylene produced with the use of nanosized catalyst ([Al]/[Zr] = 570) at 40 and 70°C, respectively. The phase structure of the polypropylene produced was a discrete tiny particle form, as shown in the Figures 10 and 11.

Most polymer particles shown in Figure 10 had a length of around 2 μm, which was about 200 times that of the original silica particle (length ~10 nm). With the increase of polymerization temperature, the average size (both length and width) of polymer particles increased significantly. Most polymer particles in Figure 11 (obtained at 70°C polymerization temperature) were much longer and wider than those shown in Figure 10 (obtained at 40°C polymerization temperature). The increase of the polymer particle size should be due to the increase of polymerization rate constant k_p with the increase of polymerization temperature. The increase of polymerization temperature

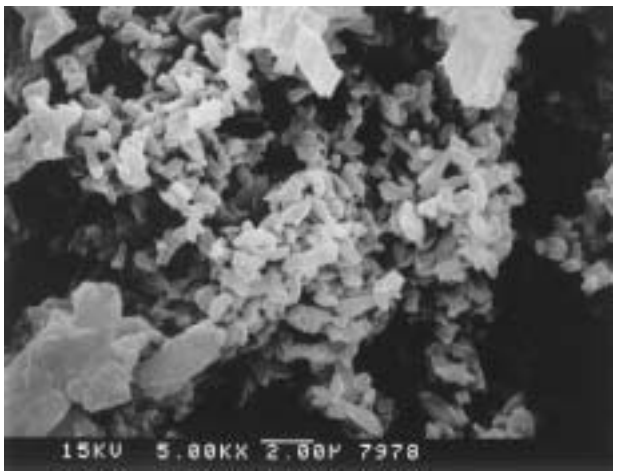

Figure 10 SEM micrograph of the polypropylene particles produced with nanosized catalyst (polymerization temperature = 40°C).

also decreased the polymer density. The measured polymer densities decreased from 0.925 g/cm^3 at 40°C polymerization temperature to 0.911 g/cm^3 at 70°C polymerization temperature. The decrease of polymer density should be due to the decrease of polymer stereoregularity at elevated temperature, and should also contribute to the larger polymer particle observed at the higher polymerization temperature.

Figures 12 and 13 display the XRD spectra of polypropylene produced with the nanosized catalyst for [Al]/[Zr] = 570 and 17, respectively. Isotactic PP can exhibit several different crystalline forms: monoclinic α form, hexagonal β form, orthorhombic γ form, and mesomorphic (smectic) form.[24] The pattern in Figure 12 ([Al]/[Zr] = 570) exhibited the characteristics peaks of α-form (at 2θ = 14°,17°,18.6°, and 21.8°), which indicates that the polymer produced was isotactic PP with a α-form. γ-crystal phase (with a characteristic peak at 2θ = 20°) was hardly observed in Figure 12, which suggests that the polymer produced at [Al]/[Zr] = 570 was highly isotatic polypropylene because the percentage of γ-crystals increased with decreasing isotacticity and stereoregularity.[25] The XRD pattern in Figure 13 ([Al]/[Zr] = 17) is quite different from that in Figure 12 ([Al]/[Zr] = 570). Figure 13 contains a significant characteristic peak of γ-form (at 2θ = 20°), which indicates that the polymer produced with the low [Al]/[Zr] ratio ([Al]/[Zr] = 17) was a mixture of α- and γ-forms. The lower polymer

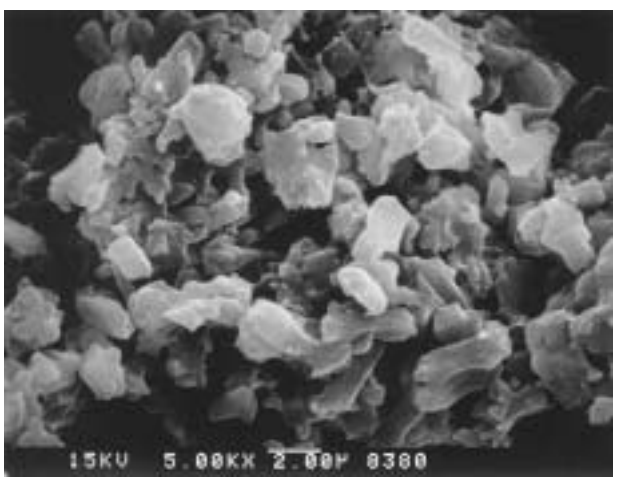

Figure 11 SEM micrograph of the polypropylene particles produced with nanosized catalyst (polymerization temperature = 70°C).

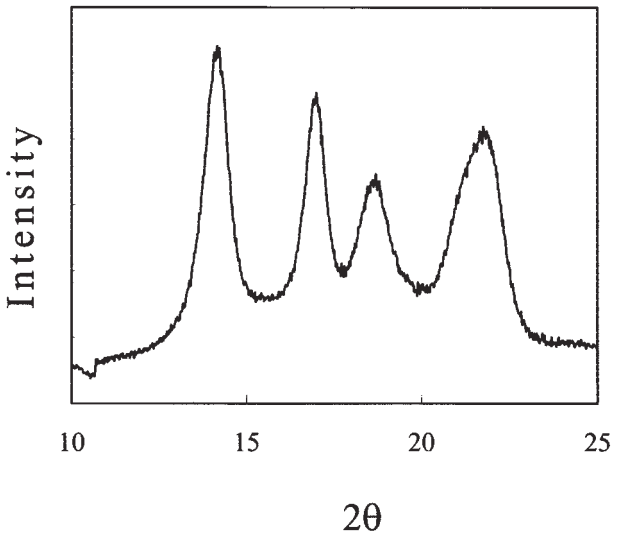

Figure 12 XRD spectra of polypropylene produced with the nanosized catalyst ([Al]/[Zr] = 570, polymerization temperature = 50°C).

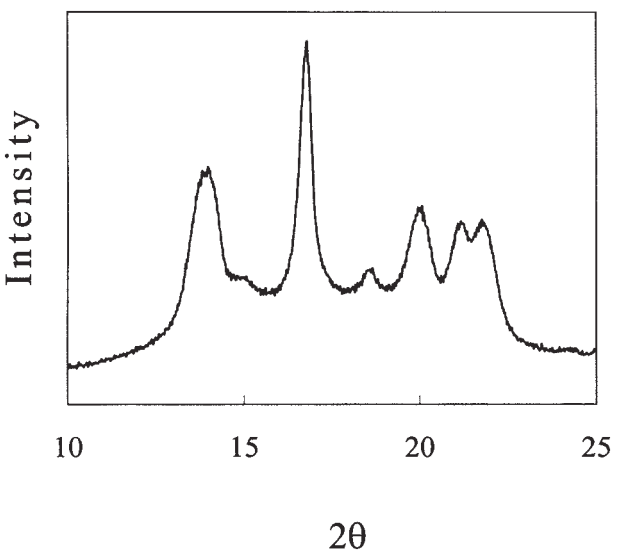

Figure 13 XRD spectra of polypropylene produced with the nanosized catalyst ([Al]/[Zr] = 17, polymerization temperature = 50°C).

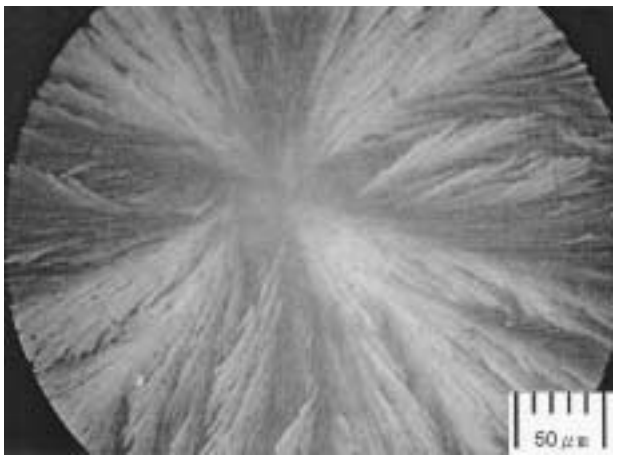

Figure 14 Morphology of a polypropylene spherulite viewed by an optical microscope with cross-polarized light, grown under isothermal conditions at 120°C.

melting points observed with the lower [Al]/[Zr] (shown in Fig. 7) should be partly due to its lower isotacticity because the percentage of γ-crystals increased with decreasing isotacticity and stereoregularity.[25]

Figure 14 shows a single spherulite grown in the melt-crystallized (crystallized isothermally at 120°C) polypropylene, which was produced by the nanosized silica supported metallocene catalyst. The spherulite structure was on the order of 370 μm and exhibited a well-defined Maltese cross appearance (in cross-polarized light) and positive optical birefringence. According to Norton and Keller's classification,[26] the spherulite in Figure 14 is Type I spherulites of isotactic plypropylene, which was formed at the temperature lower than 136°C.

CONCLUSIONS

A nanosized silica supported Et[Ind]$_2$ZrCl$_2$/MAO catalyst, containing 1.09 wt % Zr and [Al]/[Zr] = 17, has been prepared by impregnation of metallocene on a MAO-modified silica support. The influence of silica particle size, [Al]/[Zr] ratio, and polymerization temperature on the synthesis of polypropylene has been presented. The optimum polymerization temperature (in terms of polymerization activity) was 50°C. At the temperature and with [Al]/[Zr] = 570, the nanosized catalyst had a polymerization activity of 3824 kg PP/mol Zr h, which was 1.64 times that obtained with the microsized catalyst (polymerization activity was 2325 kg PP/mol Zr h). SEM studies indicated that polymer particle size increased with increasing polymerization temperature. DSC studies indicated that polymer melting point decreased with increasing polymerization temperature, but increased with increasing [Al]/[Zr] ratio. XRD studies indicated that the polymer produced was a highly crystalline isotatic polypropylene with α-form at the high [Al]/[Zr] ratio. With the decrease of [Al]/[Zr] ratio, the percentage of γ-crystals increased, indicating the decrease of isotacticity, and resulting in the decrease of the melting point.

The authors thank Mr. Fu-Sheng Ko for performing the experimental work on viscosity–average molecular weight.

References

1. Calamur, N. In Encyclopedia of Chemical Technology; Kroschwitz, J. I.; Howe-Grant, M., Eds.; Wiley: New York, 1996; Vol. 20, p 263.
2. Oertel, C. G. In Propylene Handbook; Moore, E. P., Ed.; Hanser: Munich, 1996; Chapter 10.
3. Lieberman, R. B.; Barbe, P. C. In Encyclopedia of Polymer Engineering and Science; Mark, H. F., Bikales, N. M., Overberger, C. G., Menges, G., Eds.; Wiley: New York, 1988; Vol. 13, p 464.
4. Kaminsky, W.; Kuelper, K.; Brintzinger, H. H.; Wild, F. R. W. P. Angew Chem Int Ed Engl 1985, 24, 507.
5. Kaminsky, W. J Polym Sci Part A: Polym Chem 2004, 42, 3911.
6. Soga, K.; Shiono, T. Prog Polym Sci 1997, 22, 1503.
7. Ribeiro, M. R.; Deffieux, A.; Portela, M. F. Ind Eng Chem Res 1997, 36, 1224.
8. Hlaty, G. G. Chem Rev 2000, 100, 1347.
9. Fink, G.; Steinmetz, B.; Zechlin, J.; Przyblya, C.; Tesche, B. Chem Rev 2000, 100, 1377.
10. Chien, J. C. Top Catal 1999, 7, 23.
11. Kaminsky, W.; Winkelbach, H. Top Catal 1999, 7, 61.
12. Kristen, M. O. Top Catal 1999, 7, 89.
13. Duchateau, R. Chem Rev 2002, 102, 3526.
14. Smit, M.; Zheng, X.; Loos, J.; Chadwick, J. C.; Koning, C. E. J Polym Sci Part A: Polym Chem 2005, 43, 2734.
15. Kaminsky, W.; Renner, F. Makromol Chem Rapid Commun 1993, 14, 239.
16. Chien, J. C.; He, D. J Polym Sci Part A: Polym Chem 1991, 29, 1603.
17. Evans, J. M. Polym Eng Sci 1973, 13, 401.
18. Chen, Y. X.; Rausch, M. D.; Chien, J. C. J Polym Sci Part A: Polym Chem 1995, 33, 2093.
19. Tanabe, K.; Misono, M.; Ono, Y.; Hattori, H. New Solid Acids and Bases; Elsevier: Amsterdam, 1989.
20. Hung, J.; Rempel, G. L. Ind Eng Chem Res 1997, 36, 1151.
21. Rieger, B.; Mu, X.; Mallin, D. T.; Rausch, M. D.; Chien, J. C. W. Macromolecules 1990, 23, 3559.
22. Resconi, L.; Cavallo, L.; Fait, A.; Piemontes, F. Chem Rev 2000, 100, 1253.
23. Busico, V.; Cipullo, R.; Cutillo, F.; Friederichs, N.; Ronca, S.; Wang, B. J Am Chem Soc 2003, 125, 12402.
24. Philips, R. A.; Wolkowicz, M. D. In Propylene Handbook; Moore, E. P., Ed.; Hanser: Munich, 1996; p 113.
25. Xu, J. T.; Guan, F. X.; Yasin, T.; Fan, Z. Q. J Appl Polym Sci 2003, 90, 3215.
26. Norton, D. R.; Keller, A. Polymer 1985, 26, 704.